Available online at www.sciencedirect.com
ScienceDirect
Tetrahedron
Tetrahedron 62 (2006) 10171–10181

Stereochemically pure α-trifluoromethyl-malic hydroxamates: synthesis and evaluation as inhibitors of matrix metalloproteinases

Margherita Moreno,[a,†] Monica Sani,[b,†] Guido Raos,[a,*] Stefano V. Meille,[a] Dorina Belotti,[c] Raffaella Giavazzi,[c] Stefano Bellosta,[d] Alessandro Volonterio[a] and Matteo Zanda[b,*]

[a]*Dipartimento di Chimica, Materiali ed Ingegneria Chimica 'G. Natta' del Politecnico di Milano, via Mancinelli 7, I-20131 Milano, Italy*
[b]*C.N.R.—Istituto di Chimica del Riconoscimento Molecolare, via Mancinelli 7, I-20131 Milano, Italy*
[c]*Dipartimento di Oncologia, Istituto di Ricerche Farmacologiche Mario Negri, via Gavazzeni 11, 24125 Bergamo, Italy*
[d]*Dipartimento di Scienze Farmacologiche, Università degli Studi di Milano, via Balzaretti 9, I-20133 Milano, Italy*

Received 21 March 2006; revised 25 July 2006; accepted 10 August 2006
Available online 1 September 2006

Abstract—The synthesis of trifluoromethyl (Tfm) analogs of known nanomolar matrix metalloproteinases (MMPs) inhibitors has been performed. The synthetic protocol is based on a moderately stereoselective aldol reaction of trifluoropyruvate with an *N*-acyl-oxazolidin-2-thione for the construction of the core α-Tfm-malic unit. Both the diastereomeric forms of the target α-Tfm-malic hydroxamates showed micromolar inhibitory potency toward MMP-2 and 9, according to zymographic tests, with a substantial drop with respect to the parent unfluorinated compounds. We also report some molecular modeling results, which provide a rationale for the experimental findings.

1. Introduction

Incorporation of fluorine into organic molecules is an effective strategy for improving and modifying their biological activity.[1] In particular, the trifluoromethyl group is recognized in medicinal chemistry as a substituent of distinctive qualities. It is, in fact, at the same time highly hydrophobic, electron rich, sterically demanding, moreover it can provide high in vivo stability, and is good mimic of several naturally occurring residues such as methyl, isopropyl, phenyl, etc.[2]

Matrix metalloproteinases (MMPs) are zinc (II)-dependent proteolytic enzymes involved in the degradation of the extracellular matrix.[3] More than 25 human MMPs have been identified so far. Loss in the regulation of their activity can result in the pathological destruction of connective tissue, a process associated with a number of severe diseases, such as cancer and arthritis. The inhibition of various MMPs has been envisaged as a strategy for the therapeutic intervention against such pathologies. To date, however, a number of drawbacks have hampered the successful exploitation of MMPs as pharmacological targets. In particular, the toxicity demonstrated by many MMPs' inhibitors in clinical trials has been ascribed to nonspecific inhibition. For example, recent work evidenced the importance of MMPs inhibitors sparing MMP-1, an enzyme thought to be responsible of the musculoskeletal side effect observed clinically with the broad-spectrum MMP inhibitor marimastat.[4]

Some years ago, Jacobson and co-workers described a new family of potent peptidomimetic hydroxamate inhibitors **A** (Fig. 1) of MMP-1, -3, and -9, bearing a quaternary α-methyl-alcoholic moiety at P1 position, and several different R^1 groups at P1′.[5] Interestingly, the other stereoisomers, including the epimers at the quaternary carbinol function, showed much lower activity, as the authors demonstrated that the hydroxamic binding function was moved away from the catalytic Zn^{2+} center. The crystal structure of the inhibitor **A** (R=CH_3) with MMP-3 (see Fig. 3) reveals several interesting features, including the presence of a hydrogen bond between the quaternary hydroxyl (H-bond donor) of **A** and the Glu-202 residue of the MMP-3 active site.[6]

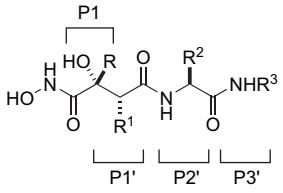

A R = CH_3; **1** R = CF_3

Figure 1.

* Corresponding authors. Tel.: +39 02 23993084; fax: +39 02 23993080 (M.Z.); e-mail addresses: guido.raos@polimi.it; matteo.zanda@polimi.it
† These authors contributed equally to the work.

0040–4020/$ - see front matter © 2006 Elsevier Ltd. All rights reserved.
doi:10.1016/j.tet.2006.08.036

Within the framework of a project aimed at studying the 'fluorine effect' in peptides and identifying selective fluorinated inhibitors of aspartic proteinases and MMPs,[8] we decided to explore the effect of the replacement of the quaternary α-methyl group in **A** with a trifluoromethyl (Tfm) group, with the hope of (1) increasing the affinity of the α-Tfm malic inhibitors with MMPs by reinforcing the α-OH hydrogen bonding, thanks to the increased acidity of the carbinolic function bearing the electron-withdrawing α-Tfm group; (2) improving the selectivity in favor of MMP-3 and -9 through the increased stereo-electronic demands of the Tfm group.

In this paper we describe in full detail the synthesis of the Tfm-analogs **1** (Fig. 1) of **A**, the effect of the replacement of the α-CH_3 group with a CF_3 on the inhibition of MMP-3 and 9, and an attempt to rationalize the experimental findings through molecular modeling.[9]

2. Results and discussion

2.1. Synthesis

We decided to concentrate our efforts on the substrates **1** having $R^1=(CH_2)_4Ph$, whose analogs **A** were reported to be very active. The α-Tfm-malic unit of **1** was recently obtained by our group via titanium (IV) catalyzed aldol reaction of trifluoropyruvic esters with enantiopure *N*-acyl oxazolidin-2-ones.[10] Although this reaction was per se satisfactory, the subsequent exocyclic cleavage of the oxazolidin-2-one auxiliary could not be performed, despite intensive efforts. We therefore decided to exploit the potential of oxazolidin-2-thiones,[11] whose cleavage has been reported to occur much more smoothly.[12]

The $TiCl_4$ catalyzed reaction of the *N*-acyl-oxazolidin-2-thione **2** (Scheme 1) with ethyl trifluoropyruvate **3** afforded the two diastereomeric adducts **4** and **5**, out of four possible, in low diastereomeric ratio. It is worth noting that the reaction features a favorable scale-up effect, affording ca. 70% yield on a hundred-milligram scale, and 90% on a ten-gram scale (the reaction was repeated many times on both scales). Several alternative conditions were explored, but no improvement in terms of diastereocontrol could be achieved. For example, with $Sn(OTf)_2/NEt_3$ and Bu_2BOTf/NEt_3 no reaction was observed, whereas LDA afforded a **4**:**5** ratio=2.6/1.0 (48% overall). However, the use of $TiCl_4$/(−)-sparteine produced a switch of diastereocontrol affording a 1.6:1.0 mixture in favor of **5**, in overall 74% yield. However, due to the cost of (−)-sparteine and the absence of a favorable scale-up effect, the $TiCl_4$/DIPEA system was always employed for conducting the reaction on a multigram scale.

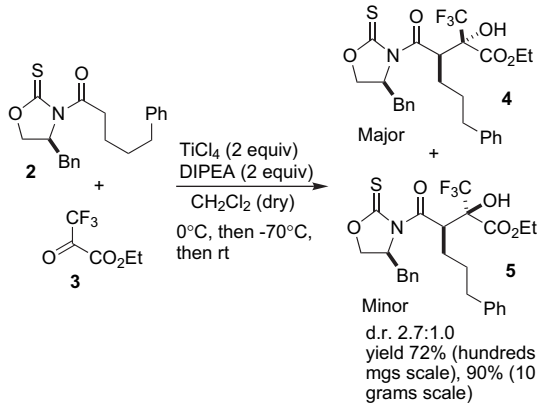

Scheme 1. The aldol reaction to form the α-Tfm-malic framework.

Cleavage of the oxazolidin-2-thione was found to be considerably more challenging than expected. In fact, under the standard conditions reported in the literature (BnOH, cat. DMAP, DCM, rt) the reaction on **4** was very slow,[12] affording modest conversion to the corresponding Bn-ester **6** (60%) after one week at reflux (Scheme 2), with partial (17%) α-epimerization to give *ent*-**7**. Even less effectively, the same reaction performed on **5** gave 56% yield of the diastereomeric Bn-ester **7**, containing 33% of the α-epimer *ent*-**6**. Although the unreacted starting materials **4** and **5** could be recovered unchanged in good yields, we felt that more efficient conditions were needed in order to complete the synthesis. Disappointingly, exploration of several different combinations of alcohols, solvents, and bases did not improve the situation.

However, we were glad to find that solid K_2CO_3 in moist dioxane (rt, 10–12 h) was able to produce directly the key carboxylic acid intermediates **8** and **9** (Scheme 3), from **4** and **5**, respectively, in satisfactory yields and with very low α-epimerization (2% for **8**, 9% for **9**).

In order to assess the stereochemistry of these compounds, the diastereomer **8** was coupled with L-Ala-$NH(CH_2)_2Ph$

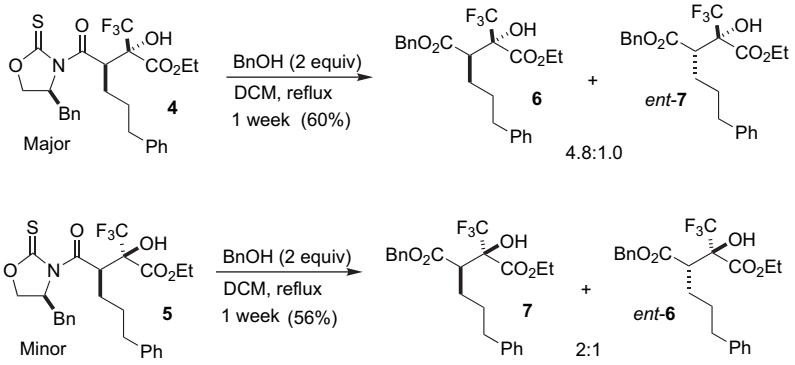

Scheme 2. Attempted oxazolidin-2-thione cleavage with BnOH.

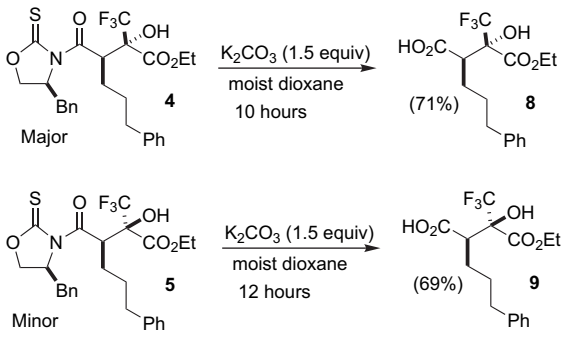

Scheme 3. Cleavage of the oxazolidin-2-thione auxiliary with K_2CO_3 in moist dioxane.

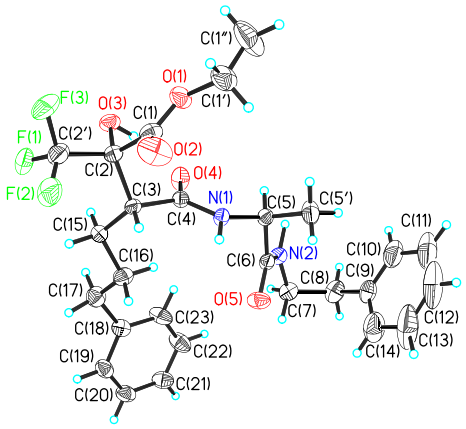

Figure 2. ORTEP view of **8x**.

(Scheme 4), affording the crystalline dipeptide **8x**, whose structure was determined by X-ray diffraction (Fig. 2).[13]

Coupling of the acid **8** with α-amino acid amides **10a–c** was achieved in good yields with the HOAt/HATU system (Scheme 5).[14] The resulting peptidomimetic esters **11a–c** were submitted to saponification, affording the acids **12a–c** in high yields. The subsequent coupling of **12a–c** with *O*-Bn hydroxylamine proved to be extremely challenging, owing to the low reactivity and high steric hindrance of the carboxylic group bound the quaternary α-Tfm carbinolic center. A number of 'conventional' coupling agents for peptides[15] were tested (among them DCC/DMAP, EDC/HOBt, DIC/HOBt, HATU/HOAt, PyBroP/DIPEA) but no trace of the target *O*-Bn hydroxamates **13a–c** could be obtained. Finally, we found that freshly prepared $BrPO(OEt)_2$ was able to promote the coupling in reasonable yields (32–61%).[16] With **13a–c** in hand we addressed the final *O*-Bn cleavage by hydrogenolysis, that provided the hydroxamates **14a–c** in good yields.

Since **14a–c** are the 'wrong' diastereomers with respect to **A**, we deemed it necessary to synthesize at least one analog having the correct stereochemistry, in order to have a complete set of biological data on the effect of the introduction of the Tfm group. However, a tailored synthetic protocol had to be developed ex-novo, because the minor diastereomer **9** (Scheme 6) featured a dramatically different reactivity in the key steps of the synthesis. First of all, we noticed that the coupling of **9** and **10a** with HATU/HOAt gave rise to relevant amounts of the β-lactone **15**, which had to be processed separately, besides the expected coupling product **16**. Thus, we decided to first prepare the intermediate **15** (72%), which could be purified by short flash chromatography (FC).

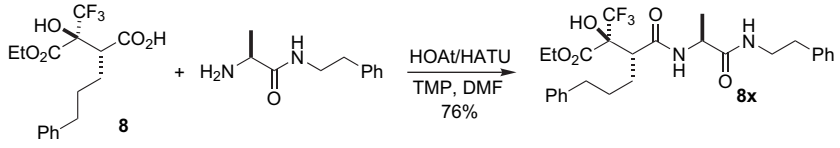

Scheme 4. Synthesis of the dipeptide **8x** for X-ray diffraction.

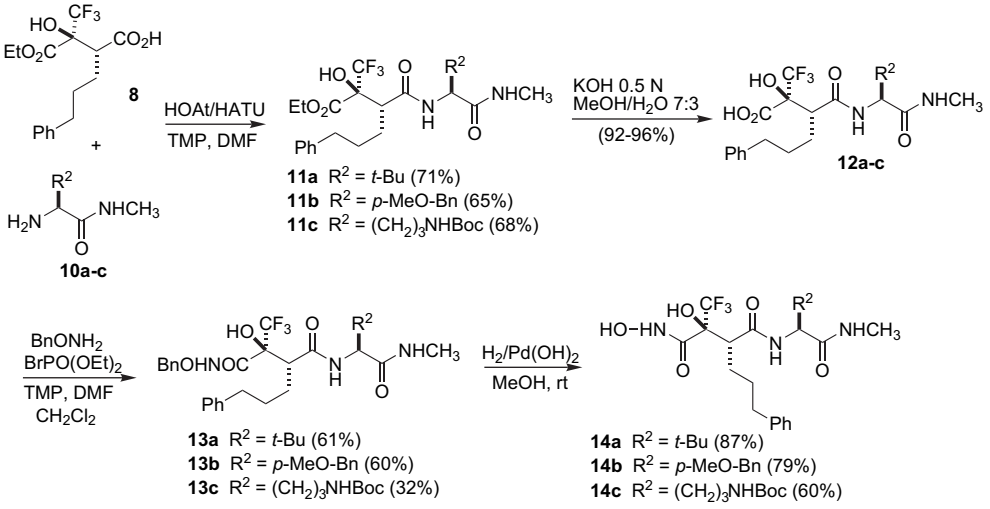

Scheme 5. Synthesis of the peptidomimetics **14** from the major diastereomer **8**.

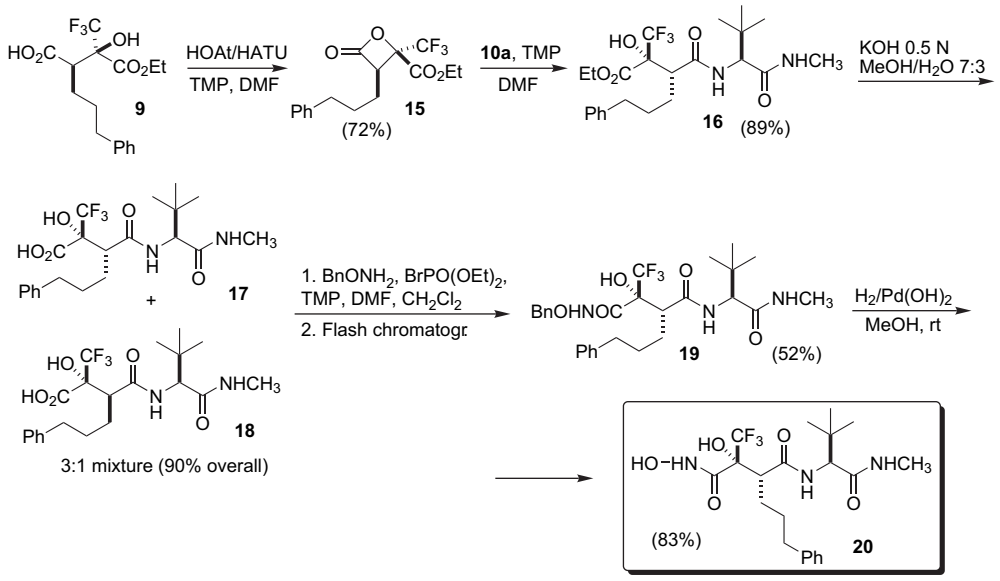

Scheme 6. Synthesis of the target peptidomimetic **20** from the minor diastereomer **9**.

The latter was reacted with free **10a**, affording the desired molecule **16** in high yields.[17]

Saponification of the ester **16** occurred effectively, but disappointingly a partial epimerization of the [Ph(CH$_2$)$_3$]-stereocenter occurred, affording a 3:1 mixture of diastereomers **17** and **18** under optimized conditions. Since their chromatographic separation proved to be difficult, **17** and **18** were subjected together to coupling with BnONH$_2$ under the previously optimized conditions. The resulting diastereomeric *O*-Bn hydroxamates could be separated by FC, affording pure **19** (52%), that was hydrogenated to the target free hydroxamate **20** in 83% yield.

The hydroxamates **14a–c** and **20** were tested for their ability to inhibit MMP-2 and MMP-9 activity using zymographic analysis. The four hydroxamates inhibited, in a dose-dependent manner, the gelatinolytic bands at 92 and 72 kDa, corresponding respectively to pro-MMP-9 and pro-MMP-2 released in the conditioned medium by human melanoma cells WM983A. The IC$_{50}$ values (μM) portrayed in Table 1 show that diastereomers **14a–c** displayed low inhibitory activity, in line with the parent CH$_3$ compounds. Disappointingly, **20** showed a much lower activity than the exact CH$_3$-analog **A**, that was reported to be a low nanomolar inhibitor of MMP-9.

Table 1. IC$_{50}$ (μM) of the target Tfm-hydroxamates

Compound	MMP-2	MMP-9
14a	156	121
14b	407	84
14c	722	23
20	23	15

It is also worth noting that **14a** and **20** showed little selectivity, whereas **14b** and **14c** showed a better affinity for MMP-9, in comparison with MMP-2.

2.2. Simulations

In an attempt to explain the different activities of the hydrogenated (**A**) and the fluorinated (**1**) compounds, we first performed molecular dynamics (MD) simulations of a few protein-inhibitor complexes. The experimental X-ray structures[5] of the complexes of **1** with MMP-3 (Fig. 3) provided a very convenient starting point for these simulations. However we found that these simulations could not clearly discriminate between the different inhibitors, since both the hydrogenated and the fluorinated ligands remained coordinated to the active site within the time of the simulation. The likely reason for this failure is the limited time span, which could be explored by MD with current computer resources (a few nanoseconds). Therefore, instead of studying the whole protein–ligand complexes, we decided to factor the problem and investigate separately the effect of fluorination on (a) the coordinating strength of the hydroxamate group and (b) non-bonded interactions and the conformational equilibrium of the ligands.

The effect of fluorination on the coordinating strength of the ligands was investigated by ab initio B3LYP/6-31G* calculations on the reactants and products of the exchange reaction shown in Figure 4 (see Section 3). After energy minimization, we computed the net reaction energy as $\Delta E = E(\text{products}) - E(\text{reactants}) = +8.8$ kJ/mol. Therefore the replacement of –CH$_3$ by –CF$_3$ reduces the coordinating ability of the hydroxamate, presumably because of the electron-withdrawing effect of the latter.

Inspection of the conformation adopted by inhibitors **A** within the active site of MMP-3 reveals that the closest non-bonded contact formed by the methyl in P1 position is an intramolecular one, with the aromatic ring of the pseudo-tyrosine at the P2′ position (see Fig. 5). Replacement of this methyl by the more sterically demanding and electron-rich Tfm might produce a change in the intramolecular conformational equilibria of the ligand, affecting as a side

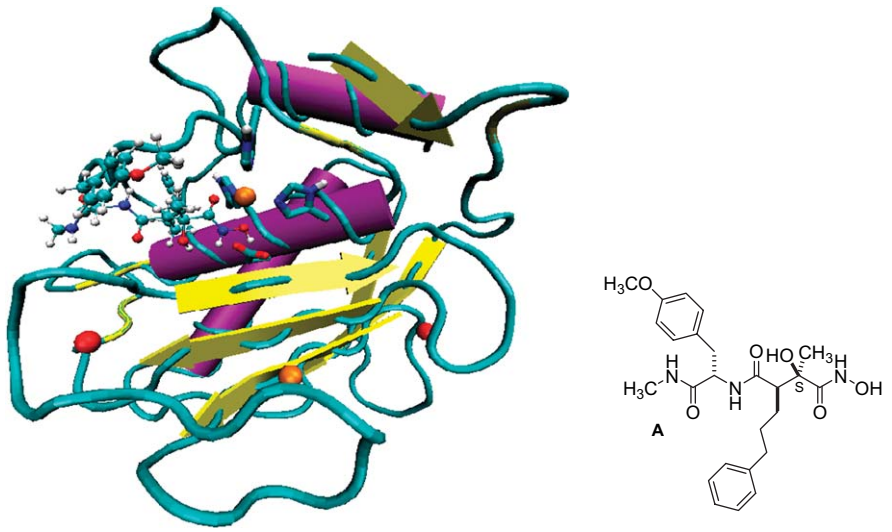

Figure 3. X-ray structure of the inhibitor **A** [R^1=$(CH_2)_3$Ph, R^2=4-CH_3O–$C_6H_4CH_2$, R^3=CH_3] bound to MMP-3 (courtesy of Bristol–Myers Squibb). The Zn^{2+} ion in the active site, the inhibitor, the three coordinating histidines, and the Glu-202 residue have been highlighted. Image produced with VMD.[7]

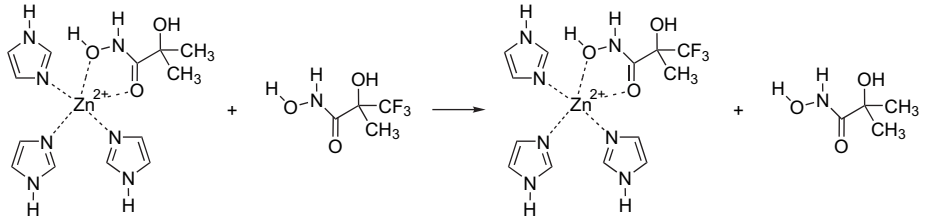

Figure 4. Exchange reaction between models of the hydrogenated and fluorinated ligands at the active site, investigated by ab initio calculations.

effect its ability to fit inside the protein active site. Therefore, we decided to carry out MD simulations of the inhibitors in water to test this hypothesis.

The analysis of a long (12 ns) MD simulation of the inhibitors in water (see Section 3 for details) produced very similar histograms for the populations of almost every torsion angle, indicating that they are mostly unaffected by fluorine substitution. However, we observed a certain difference in the populations of the C–C bond connecting the pseudo-tyrosine residue to the backbone (highlighted in yellow in Fig. 5). Therefore we decided to investigate further this point by computing the free energy profile of the molecules along this particular degree of freedom (see again Section 3). Figure 6 shows that the resulting torsion free energies are very similar, except for one important detail: the conformation at 300°, which is the one adopted by the inhibitor in the active site, is slightly destabilized by the introduction of the $–CF_3$ group. We identify this destabilization with the unfavorable interaction between the electron-rich Tfm and aromatic group. The lowest-energy conformation (by 2.5 kJ/mol) now corresponds to the state at 60°. As can be seen in Figure 5, this produces major change in the overall molecular shape.

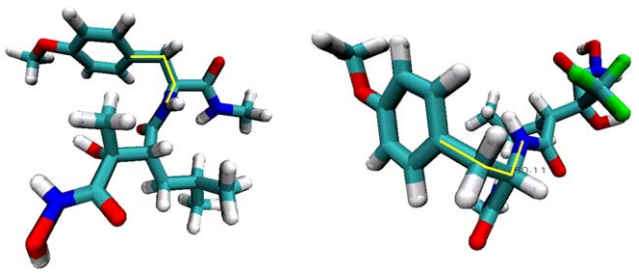

Figure 5. Minimum free energy conformations of **A** (left) and **1** (right), as obtained by MD simulations in water. With reference to Figure 1, R^1=$CH_2CH(CH_3)_2$, R^2=4-CH_3O–$C_6H_4CH_2$, R^3=CH_3. The conformation of **A** coincides with the experimental conformation within the active site. The broken yellow line indicates the torsion angle sampled in the free energy calculations. Images produced with VMD.[7]

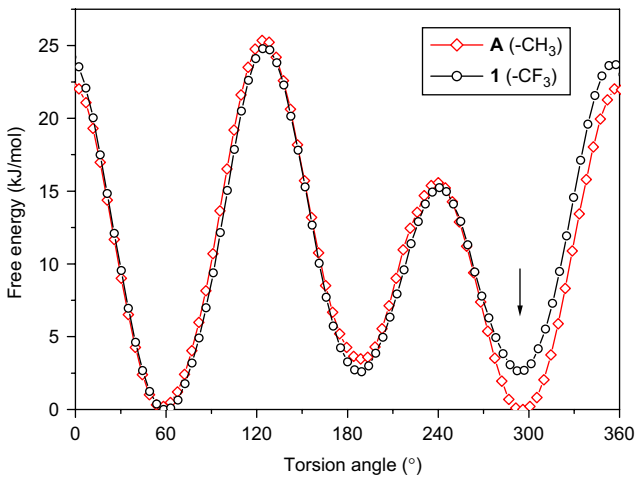

Figure 6. Free energy curves of **A** and **1** in water, corresponding to the torsion about the C–C bond connecting the pseudo-tyrosine residue to the backbone. The arrow indicates the conformation adopted inside the protein active site.

In summary, our molecular modeling study has allowed to identify two concurrent reasons for the reduced activity of the fluorinated inhibitors: (a) reduced coordinating strength of the neighboring hydroxamate group, and (b) the need of the fluorinated molecule to adopt within the binding site a conformation which does not coincide with its minimum-energy conformation in solution. Assuming additivity of these effects, we estimate that the overall binding energy of the fluorinated inhibitor to the active site is reduced by approximately 11.3 kJ/mol, compared to the original one. This results, at room temperature, in the reduction in the binding constant by two order of magnitude [$K_F/K_H = \exp\{-11.3/(0.00831 \times 298)\} = 0.010$]. This result roughly corresponds to the experimental observation.

3. Experimental

3.1. General details

Commercially available reagent-grade solvents were employed without purification. All reactions where an organic solvent was employed were performed under nitrogen atmosphere, after flame-drying of the glass apparatus. Melting points (mp) are uncorrected and were obtained on a capillary apparatus. TLC were run on silica gel 60 F_{254} Merck. Flash chromatographies (FC) were performed with silica gel 60 (60–200 μm, Merck). ^{1}H, ^{13}C, and ^{19}F NMR spectra were run at 250, 400 or 500 MHz. Chemical shifts are expressed in parts per million (δ), using tetramethylsilane (TMS) as internal standard for ^{1}H and ^{13}C nuclei (δ_H and δ_C=0.00), while C_6F_6 was used as external standard (δ_F −162.90) for ^{19}F.

3.2. Synthesis of aldol adducts 4 and 5

To a solution of *N*-acyl-oxazolidin-2-thione **2** (107 mg, 0.30 mmol) in dry CH_2Cl_2 (4 mL), cooled at 0 °C and under nitrogen atmosphere, a 1 M solution of $TiCl_4$ in toluene (600 μL, 0.60 mmol) was added. The solution was stirred for 5 min, then neat DIPEA (103 μL, 0.60 mmol) was added. The dark red solution of titanium enolate was stirred for 20 min at 0 °C, then cooled at −70 °C and neat ethyl trifluoropyruvate **3** (100 μL, 0.75 mmol) was added dropwise. The resulting mixture was stirred for 1 h at −70 °C, then warmed to rt. The reaction was quenched with a saturated aqueous NH_4Cl solution. The layers were separated and the aqueous phase was extracted with CH_2Cl_2. The collected organic phases were dried over anhydrous Na_2SO_4, filtered and the solvent was removed in vacuo. The residue was purified by FC (*n*-Hex/EtOAc 9:1), affording 59 mg of **4**, 33 mg of **5**, and 21 mg of their mixture (72% overall yield).

Compound **4**: yellow oil; R_f 0.44 (EtOAc/*n*-Hex 2:8); $[\alpha]_D^{23}$ +88.9 (*c* 1.4, $CHCl_3$); FTIR (film) ν_{max}: 3462, 1748, 1691, 1348 cm^{-1}; ^{1}H NMR (250 MHz, $CDCl_3$) δ: 7.48–7.00 (m, 10H), 6.11 (dd, *J*=7.3, 5.8 Hz, 1H), 4.76 (m, 1H), 4.44–4.14 (m, 4H), 4.11–4.00 (m, 1H), 3.23 (dd, *J*=13.1, 3.1 Hz, 1H), 2.71–2.49 (m, 3H), 2.12–1.94 (m, 2H), 1.89–1.51 (m, 2H), 1.31 (t, *J*=7.3 Hz, 3H); ^{13}C NMR (62.9 MHz, $CDCl_3$) δ: 184.5, 174.4, 168.3, 141.4, 134.9, 129.3, 129.1, 128.3, 127.5, 125.9, 123.0 (q, *J*=286.7 Hz), 78.6 (q, *J*=29.6 Hz), 69.7, 63.7, 60.5, 43.8, 37.1, 35.9, 28.4, 27.3, 13.9; ^{19}F NMR (235.3 MHz, $CDCl_3$) δ: −75.4 (s, 3F); MS (DIS EI 70 eV) *m*/*z* (%): 524 [M+H$^+$] (36), 330 (62), 194 (100); HRMS *m*/*z* 523.1630 (calculated 523.1633, $C_{26}H_{28}F_3NO_5S$).

Compound **5**: yellow oil; R_f 0.36 (EtOAc/*n*-Hex 2:8); $[\alpha]_D^{23}$ +37.3 (*c* 1.6, $CHCl_3$); FTIR (film) ν_{max}: 3467, 1747, 1693, 1498 cm^{-1}; ^{1}H NMR (250 MHz, $CDCl_3$) δ: 7.47–7.02 (m, 10H), 6.34 (dd, *J*=10.4, 3.7 Hz, 1H), 4.95 (m, 1H), 4.44–4.14 (m, 5H), 3.29 (dd, *J*=13.1 and 3.1 Hz, 1H), 2.67 (dd, *J*=13.1 and 10.4 Hz, 1H), 2.65–2.53 (m, 2H), 2.11–1.99 (m, 1H), 1.85–1.45 (m, 3H), 1.32 (t, *J*=6.9 Hz, 3H); ^{13}C NMR (62.9 MHz, $CDCl_3$) δ: 184.7, 174.3, 167.1, 141.2, 134.9, 129.3, 129.0, 128.3, 127.5, 123.2 (q, *J*=288.5 Hz), 79.1 (q, *J*=29.6 Hz), 69.8, 63.7, 59.9, 42.7, 37.0, 35.0, 28.8, 28.3, 13.8; ^{19}F NMR (235.3 MHz, $CDCl_3$) δ: −75.6 (s, 3F); MS (DIS EI 70 eV) *m*/*z* (%): 524 [M+H$^+$] (13), 330 (38), 194 (100).

3.3. Cleavage of the oxazolidin-2-thione

3.3.1. A—Cleavage with BnOH. General procedure. To a solution of **4** (102 mg, 0.19 mmol) in CH_2Cl_2 (5 mL), neat BnOH (40 μL, 0.38 mmol) and DMAP (4.2 mg, 0.038 mmol) were added. The solution was refluxed for one week. The solvent was removed in vacuo and the crude was purified by FC (*n*-Hex/EtOAc 9:1), affording 30 mg of **6**, 5 mg of *ent*-**7**, and 15 mg of their mixture (60% overall yield).

Compound **6**: colorless oil; R_f 0.25 (EtOAc/*n*-Hex 1:9); $[\alpha]_D^{23}$ +7.9 (*c* 0.9, $CHCl_3$); FTIR (film) ν_{max}: 3741, 1748, 1456 cm^{-1}; ^{1}H NMR (250 MHz, $CDCl_3$) δ: 7.41–6.99 (m, 10H), 5.08 (s, 2H), 4.23–3.99 (m, 3H), 3.26 (dd, *J*=9.4, 4.5 Hz, 1H), 2.64–2.53 (m, 2H), 2.02–1.46 (m, 4H), 1.24 (t, *J*=6.6 Hz, 3H); ^{13}C NMR (62.9 MHz, $CDCl_3$) δ: 171.1, 168.9, 141.7, 134.9, 128.6, 128.5, 128.3, 123.1 (q, *J*=288.4 Hz), 78.1 (q, *J*=29.6 Hz), 67.1, 63.8, 47.7, 35.6, 29.2, 25.8, 13.6; ^{19}F NMR (235.3 MHz, $CDCl_3$) δ: −75.1 (s, 3F); MS (DIS EI 70 eV) *m*/*z* (%): 439 [M+H$^+$] (54), 117 (78), 91 (100); HRMS *m*/*z* 438.1649 (calculated 438.1647, $C_{23}H_{25}F_3O_5$).

Compound **7**: colorless oil; R_f 0.20 (EtOAc/*n*-Hex 1:9); $[\alpha]_D^{23}$ −3.8 (*c* 1.4, $CHCl_3$); FTIR (film) ν_{max}: 3467, 1746, 1456 cm^{-1}; ^{1}H NMR (250 MHz, $CDCl_3$) δ: 7.29–6.99 (m, 10H), 5.21 (d, *J*=12.0 Hz, 1H), 5.11 (d, *J*=12.0 Hz, 1H), 4.47 (s, 1H), 4.35–4.20 (m, 2H), 3.21 (dd, *J*=11.7, 3.4 Hz, 1H), 2.56 (m, 2H), 2.07–1.87 (m, 1H), 1.65–1.29 (m, 3H), 1.24 (t, *J*=6.8 Hz, 3H); ^{13}C NMR (62.9 MHz, $CDCl_3$) δ: 171.9, 167.2, 141.2, 134.9, 128.6, 128.3, 128.2, 125.9, 123.1 (q, *J*=288.5 Hz), 78.5 (q, *J*=27.7 Hz), 67.4, 63.7, 46.9, 35.1, 28.6, 27.1, 13.8; ^{19}F NMR (235.3 MHz, $CDCl_3$) δ: −76.9 (s, 3F); MS (DIS EI 70 eV) *m*/*z* (%): 439 [M+H$^+$] (59), 421 (100).

3.3.2. B—Cleavage with K_2CO_3. General procedure. To a solution of **4** (91 mg, 0.17 mmol) in moist dioxane (2 mL), K_2CO_3 (70 mg, 0.51 mmol) was added. The resulting mixture was stirred for 10 h. The solvent was removed in vacuo and the crude was dissolved in EtOAc. A 1 M solution of HCl was added until pH 1–2 was reached. The layers were separated and the aqueous phase was extracted with EtOAc. The collected organic phases were dried over anhydrous

Na_2SO_4, filtered and the solvent was removed in vacuo to give 42 mg of **8** (71% yield).

Compound **8**: colorless oil; R_f 0.48 ($CHCl_3$/MeOH 8:2); $[\alpha]_D^{23}$ +16.5 (*c* 1.4, MeOH); FTIR (film) ν_{max}: 3466.6, 1732.9, 1454.5 cm^{-1}; ^1H NMR (400 MHz, CD_3OD) δ: 7.29–7.05 (m, 5H), 4.25 (q, *J*=7.5 Hz, 2H), 3.13 (m, 1H), 2.71–2.53 (m, 2H), 1.95–1.52 (m, 4H), 1.27 (t, *J*=7.5 Hz, 3H); ^{13}C NMR (100.6 MHz, CD_3OD) δ: 177.0, 168.9, 141.5, 128.3, 128.2, 125.9, 122.9 (q, *J*=288.5 Hz), 77.9 (q, *J*=29.6 Hz), 64.2, 47.8, 35.6, 29.2, 25.7, 13.6; ^{19}F NMR (235.5 MHz, CD_3OD) δ: −75.6 (s, 3F); MS (DIS EI 70 eV) *m/z* (%): 349 [M+H$^+$] (65), 330 (60), 91 (100); HRMS *m/z* 348.1200 (calculated 348.1198, $C_{16}H_{19}F_3O_5$).

Compound **9**: colorless oil; R_f 0.46 ($CHCl_3$/MeOH 8:2); $[\alpha]_D^{23}$ +11.9 (*c* 0.9, MeOH); FTIR (film) ν_{max}: 3476, 1748, 1454 cm^{-1}; ^1H NMR (400 MHz, CD_3OD) δ: 7.28–7.09 (m, 5H), 4.29–4.15 (m, 2H), 3.05 (dd, *J*=11.7, 3.2 Hz, 1H), 2.61 (dt, *J*=7.2, 2.0 Hz, 2H), 1.97–1.85 (m, 1H), 1.76–1.59 (m, 2H), 1.44–1.32 (m, 1H), 1.21 (t, *J*=7.2 Hz, 3H); ^{13}C NMR (100.6 MHz, CD_3OD) δ: 174.8, 168.7, 141.8, 129.4, 126.9, 124.8 (q, *J*=282.6 Hz), 80.4 (q, *J*=27.7 Hz), 64.1, 49.2, 36.2, 30.2, 27.8, 14.2; ^{19}F NMR (235.3 MHz, CD_3OD) δ: −74.1 (s, 3F); MS (DIS EI 70 eV) *m/z* (%): 349 [M+H$^+$] (5), 330 (18), 159 (40), 91 (100).

3.4. Synthesis of peptidomimetics esters 11a–c and 8x. General procedure

To a solution of **8** (198 mg, 0.57 mmol) and **10a** (98 mg, 0.68 mmol) in dry DMF (5 mL), HOAt (77 mg, 0.57 mmol), HATU (217 mg, 0.57 mmol), and TMP (150 μL, 1.14 mmol) were added. The solution was stirred for 2 h, then diluted with H_2O. The resulting mixture was extracted with Et_2O and the organic phase was washed with a 1 M solution of HCl and with brine. After drying over anhydrous Na_2SO_4, and filtration, the solvent was removed in vacuo, and the residue was purified by FC (*n*-Hex/EtOAc 6:4) to give 192 mg of **11a** (71% yield), as a white solid: R_f 0.67 (EtOAc/*n*-Hex 6:4); $[\alpha]_D^{23}$ +4.5 (*c* 1.8, $CHCl_3$); FTIR (microscope) ν_{max}: 3307, 1754, 1647, 1535 cm^{-1}; ^1H NMR (400 MHz, $CDCl_3$) δ: 7.29–7.19 (m, 2H), 7.18–7.07 (m, 3H), 6.70 (br d, *J*=9.3 Hz, 1H), 6.03, (br s, 1H), 4.92 (br s, 1H), 4.33–4.17 (m, 2H), 4.14 (d, *J*=9.3 Hz, 1H), 3.08 (dd, *J*=9.3, 5.9 Hz, 1H), 2.72 (d, *J*=4.6 Hz, 3H), 2.70–2.52 (m, 2H), 1.93–1.79 (m, 2H), 1.61 (m, 2H), 1.27 (t, *J*=7.2 Hz, 3H), 0.94 (s, 9H); ^{13}C NMR (100.6 MHz, $CDCl_3$) δ: 171.5, 170.5, 168.7, 141.5, 128.4, 128.2, 125.9, 122.9 (q, *J*= 285.9 Hz), 78.9 (q, *J*=28.9 Hz), 63.6, 60.8, 49.1, 35.7, 34.5, 28.7, 26.6, 26.4, 26.1, 13.8; ^{19}F NMR (235.3 MHz, $CDCl_3$) δ: −74.5 (s, 3F); MS (DIS EI 70 eV) *m/z* (%): 474 [M$^+$] (8), 416 (18), 86 (100); HRMS *m/z* 474.2340 (calculated 474.2333, $C_{23}H_{33}F_3N_2O_5$).

Compound **11b**: white solid; R_f 0.42 (EtOAc/*n*-Hex 6:4); $[\alpha]_D^{23}$ +2.9 (*c* 1.2, in $CHCl_3$); FTIR (microscope) ν_{max}: 3300, 1745, 1650, 1517.1 cm^{-1}; ^1H NMR (400 MHz, $CDCl_3$) δ: 7.29–7.21 (m, 2H), 7.19–7.00 (m, 6H), 6.79 (d, *J*=8.8 Hz, 2H), 6.68 (br d, *J*=7.7 Hz, 1H), 5.80 (br s, 1H), 4.47 (q, *J*=7.2 Hz, 1H), 4.33–4.19 (m, 2H), 3.72 (s, 3H), 3.04 (dd, *J*=10.9, 4.4 Hz, 1H), 2.90 (dd, *J*=13.7, 7.2 Hz, 1H), 2.88 (dd, *J*=13.7, 7.2 Hz, 1H), 2.67 (d, *J*=4.9 Hz, 3H), 2.63–2.46 (m, 2H), 1.86–1.65 (m, 2H), 1.52–1.39 (m, 2H), 1.28 (t, *J*=7.2 Hz, 3H); ^{13}C NMR (100.6 MHz, $CDCl_3$) δ: 171.2, 170.7, 169.2, 158.8, 141.5, 130.1, 128.4, 128.3, 128.2, 125.9, 122.8 (q, *J*=287.5 Hz), 114.3, 78.5 (q, *J*=29.3 Hz), 64.0, 55.2, 54.8, 49.3, 37.3, 35.5, 28.6, 26.2, 13.8; ^{19}F NMR (235.3 MHz, $CDCl_3$) δ: −74.3 (s, 3F); MS (DIS EI 70 eV) *m/z* (%): 539 [M+H$^+$] (34), 191 (100); HRMS *m/z* 538.2281 (calculated 538.2282, $C_{27}H_{33}F_3N_2O_6$).

Compound **11c**: white solid; R_f 0.19 (AcOEt/*n*-Hex 1:1); $[\alpha]_D^{23}$ +13.9 (*c* 0.84, $CHCl_3$); FTIR (microscope) ν_{max}: 3284, 1750, 1639, 1531 cm^{-1}; ^1H NMR (250 MHz, $CDCl_3$) δ: 7.43 (br s, 1H), 7.35–7.08 (m, 5H), 7.02 (br s, 1H), 5.01 (br s, 1H), 4.59 (br s, 1H), 4.38–4.19 (m, 2H), 3.46–3.25 (m, 1H), 3.18 (dd, *J*=10.8, 4.2 Hz, 1H), 3.13–2.95 (m, 1H), 2.74 (d, *J*=4.4 Hz, 3H), 2.69–2.54 (m, 2H), 2.03–1.70 (m, 4H), 1.69–1.56 (m, 2H), 1.46 (s, 9H), 1.31 (t, *J*=6.8 Hz, 3H); ^{13}C NMR (62.9 MHz, $CDCl_3$) δ: 171.9, 171.6, 168.8, 156.7, 141.5, 128.4, 128.2, 125.7, 122.9 (q, *J*=286.7 Hz), 78.9 (q, *J*=29.6 Hz), 63.2, 48.3, 35.5, 28.6, 28.3, 25.9, 13.7; ^{19}F NMR (235.3 MHz, $CDCl_3$) δ: −74.2 (s, 3F); MS (DIS EI 70 eV) *m/z* (%): 576 [M+H$^+$] (20), 474 (30), 430 (60), 57 (100); HRMS *m/z* 575.2811 (calculated 575.2808, $C_{27}H_{40}F_3N_3O_7$).

Compound **8x**: white solid; R_f 0.29 (AcOEt/*n*-Hex 4:6); $[\alpha]_D^{23}$ −10.4 (*c* 1.2, $CHCl_3$); mp=93–97 °C (EtOAc/*n*-Hex); FTIR (microscope) ν_{max}: 3280, 1752, 1641, 1533.5 cm^{-1}; ^1H NMR (250 MHz, $CDCl_3$) δ: 7.37–7.11 (m, 10H), 6.53 (d, *J*=7.9 Hz, 1H), 5.96 (br t, *J*=5.3 Hz, 1H), 4.36–4.22 (m, 3H), 3.59–3.43 (m, 2H), 3.04 (dd, *J*=11.2, 5.3 Hz, 1H), 3.87–2.77 (m, 2H), 2.73–2.57 (m, 2H), 1.94–1.82 (m, 2H), 1.79–1.68 (br s, 1H), 1.67–1.57 (m, 2H), 1.33 (t, *J*=7.2 Hz, 3H), 1.27 (d, *J*=6.6 Hz, 3H); ^{13}C NMR (62.9 MHz, $CDCl_3$) δ: 171.4, 170.7, 168.8, 141.5, 138.4, 128.7, 128.6, 128.3, 128.2, 126.5, 125.9, 123.0 (q, *J*=286.7 Hz), 78.6 (q, *J*=29.5 Hz), 63.6, 48.7, 40.7, 35.5, 35.3, 28.7, 25.8, 18.4, 13.8; ^{19}F NMR (235.3 MHz, $CDCl_3$) δ: −73.8 (s, 3F); MS (DIS EI 70 eV) *m/z* (%): 576 [M+H$^+$] (20), 474 (30), 430 (60), 57 (100). Anal. Calcd for $C_{27}H_{33}F_3N_2O_5$: C, 62.06; H, 6.37; N, 5.36. Found: C, 61.98; H, 6.44; N, 5.31.

3.5. Synthesis of acids 12a–c. General procedure

To a solution of **11a** (123 mg, 0.26 mmol) in a MeOH/H_2O 7:3 mixture (5 mL), a 0.5 M aqueous solution of KOH (1.00 mL, 0.52 mmol) was added. The reaction was stirred for 2 h, then the MeOH was removed in vacuo. A 1 M solution of HCl was added until pH 1–2 was reached, and the reaction mixture was extracted with EtOAc. The organic phase was dried over anhydrous Na_2SO_4, filtered and the solvent was removed in vacuo to give 111 mg of **12a** (96% yield), as a white solid: R_f 0.54 ($CHCl_3$/MeOH 7:3); $[\alpha]_D^{23}$ +1.3 (*c* 1.2, MeOH); FTIR (microscope) ν_{max}: 3453, 1749, 1654, 1488 cm^{-1}; ^1H NMR (400 MHz, CD_3OD) δ: 7.30–7.06 (m, 5H), 4.19 (s, 1H), 3.23 (dd, *J*=10.3, 4.7 Hz, 1H), 2.64 (s, 4H), 2.59–2.50 (m, 1H), 1.85–1.74 (m, 2H), 1.68–1.51 (m, 2H), 0.97 (s, 9H); ^{13}C NMR (100.6 MHz, CD_3OD) δ: 174.1, 172.6, 170.8, 141.5, 128.4, 128.2, 125.9, 122.9 (q, *J*=285.9 Hz), 78.9 (q, *J*=28.9 Hz), 63.6, 35.7, 34.5, 28.7, 26.6, 26.4, 26.1, 13.8; ^{19}F NMR (250 MHz, CD_3OD) δ: −74.5 (s, 3F); MS (DIS EI 70 eV) *m/z* (%): 447 [M+H$^+$]

(8), 388 (20), 91 (40), 86 (100); HRMS *m/z* 446.2018 (calculated 446.2021, $C_{21}H_{29}F_3N_2O_5$).

Compound **12b**: white solid; R_f 0.45 ($CHCl_3$/MeOH 7:3); $[\alpha]_D^{23}$ +4.2 (*c* 0.3, MeOH); FTIR (microscope) ν_{max}: 3371, 1743, 1654, 1434 cm^{-1}; ^1H NMR (400 MHz, CD_3OD) δ: 7.29–7.19 (m, 2H), 7.17–7.03 (m, 5H), 6.81 (d, *J*=8.9 Hz, 2H), 4.51 (t, *J*=7.2 Hz, 1H), 3.70 (s, 3H), 3.06–2.98 (m, 2H), 2.86 (dd, *J*=14.1, 7.9 Hz, 1H), 2.64 (s, 3H), 2.61–2.41 (m, 2H), 1.79–1.60 (m, 2H), 1.48–1.36 (m, 2H); ^{13}C NMR (100.6 MHz, CD_3OD) δ: 173.6, 170.6, 169.9, 158.9, 141.2, 130.2, 128.4, 128.3, 127.6, 126.0, 123.0 (q, *J*=284.7 Hz), 114.3, 77.6 (q, *J*=28.9 Hz), 55.8, 55.3, 48.1, 37.7, 35.2, 28.4, 27.4, 26.2; ^{19}F NMR (235.3 MHz, CD_3OD) δ: −72.5 (s, 3F); MS (DIS EI 70 eV) *m/z* (%): 511 [M+H$^+$] (15), 209 (20), 191 (100); HRMS *m/z* 510.1965 (calculated 510.1970, $C_{25}H_{29}F_3N_2O_6$).

Compound **12c**: white solid; R_f 0.27 ($CHCl_3$/MeOH 8:2); $[\alpha]_D^{23}$ −1.9 (*c* 1.1, MeOH); FTIR (microscope) ν_{max}: 3302, 1746, 1656, 1522 cm^{-1}; ^1H NMR (250 MHz, CD_3OD) δ: 7.30–7.07 (m, 5H), 4.38–4.25 (m, 1H), 3.16–2.98 (m, 3H), 2.68 (s, 3H), 2.65–2.48 (m, 2H), 1.89–1.55 (m, 8H), 1.42 (s, 9H); ^{13}C NMR (62.9 MHz, CD_3OD) δ: 174.9, 171.8, 159.5, 144.1, 130.4, 130.2, 127.7, 125.8 (q, *J*=286.7 Hz), 80.7 (q, *J*=29.6 Hz), 62.4, 55.2, 41.5, 37.4, 31.1, 29.7, 28.6, 28.3, 27.2; ^{19}F NMR (235.3 MHz, CD_3OD) δ: −72.5 (s, 3F); MS (DIS EI 70 eV) *m/z* (%): 548 [M+H$^+$] (5), 430 (60), 41 (100); HRMS *m/z* 547.2499 (calculated 547.2496, $C_{25}H_{36}F_3N_3O_7$).

3.6. Synthesis of lactone 15

To a solution of **9** (50 mg, 0.14 mmol) in DMF (2 mL), HOAt (20 mg, 0.15 mmol), HATU (57 mg, 0.15 mmol), and TMP (37 μL, 0.28 mmol) were added. The solution was stirred for 2 h, then diluted with H_2O. The resulting mixture was extracted with Et_2O and the organic phase was washed with a 1 M solution of HCl and with brine. After drying over anhydrous Na_2SO_4, and filtration, the solvent was removed in vacuo, and the residue was purified by FC (*n*-Hex/(*i*Pr)$_2$O 9:1) to give 33 mg of **15** (72% yield) as a colorless oil: R_f 0.55 (EtOAc/*n*-Hex 1:9); $[\alpha]_D^{23}$ +6.8 (*c* 0.8, $CHCl_3$); FTIR (film) ν_{max}: 1870, 1752, 1454 cm^{-1}; ^1H NMR (400 MHz, $CDCl_3$) δ: 7.35–7.09 (m, 5H), 4.31 (q, *J*=7.2 Hz, 2H), 3.99 (m, 1H), 2.73–2.58 (m, 2H), 1.90–1.69 (m, 4H), 1.30 (t, *J*=7.2 Hz, 3H); ^{13}C NMR (100.6 MHz, $CDCl_3$) δ: 165.5, 162.4, 140.7, 128.6, 128.4, 121.9 (q, *J*=281.4 Hz), 76.5 (q, *J*=33.7 Hz), 63.6, 58.0, 35.2, 28.1, 24.8, 13.9; ^{19}F NMR (235.3 MHz, $CDCl_3$) δ: −77.1 (s, 3F); MS (DIS EI 70 eV) *m/z* (%): 330 [M$^+$] (17), 159 (40), 104 (100); HRMS *m/z* 330.1079 (calculated 330.1074, $C_{16}H_{17}F_3O_4$).

3.7. Synthesis of peptidomimetic ester 16

To a solution of **15** (139 mg, 0.42 mmol) and **10a** (121 mg, 0.84 mmol) in DMF (5 mL), TMP (111 μL, 0.84 mmol) was added. The solution was stirred for 6 h, then diluted with H_2O. The resulting mixture was extracted with Et_2O and the organic phase was washed with a 1 M solution of HCl, then with brine. After drying over anhydrous Na_2SO_4 and filtration, the solvent was removed in vacuo, and the residue was purified by FC (*n*-Hex/EtOAc 7:3) to give 177 mg of **16** (89% yield) as a colorless oil: R_f 0.61 (EtOAc/*n*-Hex 1:1); $[\alpha]_D^{23}$ −0.5 (*c* 1.1, MeOH); FTIR (film) ν_{max}: 3317, 1750, 1654, 1545 cm^{-1}; ^1H NMR (400 MHz, CD_3OD) δ: 7.27–7.05 (m, 5H), 4.24–4.19 (m, 3H), 3.17 (dd, *J*=11.4, 3.5 Hz, 1H), 2.65 (s, 3H), 2.47–2.54 (m, 2H), 1.96–1.74 (m, 1H), 1.59 (m, 2H), 1.38–1.28 (m, 1H), 1.22 (t, *J*=6.9 Hz, 3H), 0.98 (s, 9H); ^{13}C NMR (100.6 MHz, CD_3OD) δ: 173.9, 172.7, 168.4, 142.9, 129.5, 129.3, 126.9, 125.1 (q, *J*=287.9 Hz), 80.5 (q, *J*=28.1 Hz), 64.0, 62.1, 47.9, 36.3, 35.2, 29.6, 29.1, 27.1, 25.9, 14.2; ^{19}F NMR (235.3 MHz, CD_3OD) δ: −73.9 (s, 3F); MS (DIS EI 70 eV) *m/z* (%): 475 [M+H$^+$] (28), 416 (20), 86 (100); HRMS *m/z* 474.2330 (calculated 474.2333, $C_{23}H_{33}F_3N_2O_5$).

3.8. Synthesis of acids 17 and 18

To a solution of **16** (278 mg, 0.59 mmol) in a MeOH/H_2O 7:3 mixture (5 mL), a 0.5 M aqueous solution of KOH (3.5 mL, 1.77 mmol) was added. The reaction was stirred for 20 h, then the MeOH was removed in vacuo. A 1 M solution of HCl was added until pH 1–2 was reached, and the reaction mixture was extracted with EtOAc. The organic phase was dried over anhydrous Na_2SO_4, filtered and the solvent was removed in vacuo to give 237 mg of a mixture of **17** and **18** (90% overall yield) as a white solid: R_f 0.37 ($CHCl_3$/MeOH 8:2); $[\alpha]_D^{23}$ −3.9 (*c* 0.8, MeOH); FTIR (microscope) ν_{max}: 3450, 1748, 1656, 1544 cm^{-1}; ^1H NMR (400 MHz, CD_3OD) δ: 7.28–7.08 (m, 5H), 4.19 (s, 1H), 3.23–3.16 (m, 1H), 2.71 (s, 3H), 2.68–2.50 (m, 2H), 1.89–1.53 (m, 4H), 0.97 (s, 9H); ^{13}C NMR (62.9 MHz, CD_3OD) δ: 175.0, 172.3, 169.1, 143.0, 129.3, 126.6, 125.2 (q, *J*=286.6 Hz), 79.8 (q, *J*=27.3 Hz), 62.2, 36.5, 35.9, 35.1, 30.6, 29.9, 26.9, 26.0; ^{19}F NMR (235.3 MHz, CD_3OD) δ: −72.9 (s, 3F); MS (DIS EI 70 eV) *m/z* (%): 447 [M+H$^+$] (25), 388 (30), 91 (40), 86 (100).

3.9. Synthesis of peptidomimetics 13a–c and 19. General procedure

To a solution of **12a** (58 mg, 0.13 mmol) in a CH_2Cl_2/DMF 2:1 mixture (3 mL), cooled at 0 °C, a solution of $BrPO(OEt)_2$ (35 mg, 0.16 mmol) in CH_2Cl_2 (0.5 mL) and neat TMP (34 μL, 0.26 mmol) were added dropwise. The resulting solution was stirred for 45 min at 0 °C, then a solution of $BnONH_2$ (32 mg, 0.26 mmol) in CH_2Cl_2 (0.5 mL) and neat TMP (34 μL, 0.26 mmol) were added. The reaction was allowed to warm to rt and stirred for 5 h. The solvent was removed in vacuo and the crude material was dissolved in a EtOAc/Et_2O 1:1 mixture. The resulting mixture was washed with a 1 M solution of HCl and with brine, then the organic phase was dried over anhydrous Na_2SO_4, filtered and the solvent was removed in vacuo. The residue was purified by FC (*n*-Hex/EtOAc 6:4) to give 44 mg of **13a** (61% yield) as a white solid: R_f 0.26 (EtOAc/*n*-Hex 3:7); $[\alpha]_D^{23}$ −23.9 (*c* 1.9, $CHCl_3$); FTIR (microscope) ν_{max}: 3228, 1692, 1646, 1537 cm^{-1}; ^1H NMR (400 MHz, $CDCl_3$) δ: 9.02 (br s, 1H), 7.46–6.96 (m, 11H), 5.84 (d, *J*=4.6 Hz, 1H), 5.69 (br s, 1H), 4.86 (s, 2H), 4.14 (d, *J*=9.6 Hz, 1H), 3.10 (dd, *J*=10.8, 3.9 Hz, 1H), 2.67 (d, *J*=4.6 Hz, 3H), 2.60–2.43 (m, 2H), 1.81–1.61 (m, 2H),1.58–1.39 (m, 2H), 0.96 (s, 9H); ^{13}C NMR (100.6 MHz, $CDCl_3$) δ: 172.9, 170.2, 163.8, 141.5, 134.8, 129.2, 128.8, 128.6, 128.3, 125.9, 123.2 (q, *J*=286.7 Hz), 78.3, 77.8 (q, *J*=28.9 Hz),

61.3, 48.2, 35.4, 34.5, 28.5, 27.1, 26.5, 26.0; ^{19}F NMR (235.3 MHz, $CDCl_3$) δ: −76.4 (s, 3F); MS (DIS EI 70 eV) *m/z* (%): 552 [M+H$^+$] (12), 370 (19), 91 (99), 86 (100); HRMS *m/z* 551.2599 (calculated 551.2598, $C_{28}H_{36}F_3N_3O_5$).

Compound **13b**: white solid; R_f 0.44 (EtOAc/*n*-Hex 1:1); $[\alpha]_D^{23}$ −14.8 (*c* 1.6, $CHCl_3$); FTIR (microscope) ν_{max}: 3245, 1657, 1567, 1423 cm^{-1}; ^{1}H NMR (400 MHz, $CDCl_3$) δ: 11.39 (br s, 1H), 7.48–7.02 (m, 13H), 6.84 (d, *J*=8.6 Hz, 2H), 5.49 (br s, 1H), 5.28 (br s, 1H), 4.93 (d, *J*=12.4 Hz, 1H), 4.87 (d, *J*=12.4 Hz, 1H), 4.06 (m, 1H), 3.77 (s, 3H), 3.05–2.93 (m, 2H), 2.81 (dd, *J*=13.7, 9.2 Hz, 1H), 2.60 (d, *J*=4.8 Hz, 3H), 2.58–2.47 (m, 2H), 1.82–1.57 (m, 2H), 1.55–1.43 (m, 2H); ^{13}C NMR (100.6 MHz, $CDCl_3$) δ: 172.6, 170.3, 163.5, 158.9, 141.5, 134.8, 130.3, 129.3, 128.9, 128.6, 128.4, 128.3, 128.2, 125.9, 123.1 (q, *J*=287.1 Hz), 114.3, 78.4 (q, *J*=27.8 Hz), 55.6, 55.3, 48.4, 37.6, 35.5, 28.8, 26.9, 26.2; ^{19}F NMR (235.3 MHz, $CDCl_3$) δ: −76.9 (s, 3F); MS (DIS EI 70 eV) *m/z* (%): 616 [M+H$^+$] (18), 191 (100); HRMS *m/z* 615.2551 (calculated 615.2547, $C_{32}H_{36}F_3N_3O_6$).

Compound **13c**: white solid; R_f 0.24 (EtOAc/*n*-Hex 1:1); $[\alpha]_D^{23}$ −27.4 (*c* 1.9, $CHCl_3$); FTIR (microscope) ν_{max}: 3368, 1688, 1653, 1412 cm^{-1}; ^{1}H NMR (400 MHz, $CDCl_3$) δ: 11.29 (br s, 1H), 7.68 (br s, 1H), 7.48–7.04 (m, 10H), 6.55 (br s, 1H), 5.61 (br s, 1H), 4.91 (m, 2H), 4.57 (br s, 1H), 4.12 (m, 1H), 3.23 (m, 1H), 3.09 (m, 1H), 2.97 (m, 1H), 2.73 (s, 3H), 2.63–2.49 (m, 2H), 1.71–1.55 (m, 7H), 1.47 (s, 10H); ^{13}C NMR (100.6 MHz, $CDCl_3$) δ: 172.9, 171.6, 163.9, 156.8, 141.5, 134.5, 129.2, 128.5, 128.2, 125.8, 123.2 (q, *J*=288.5 Hz), 79.2, 77.5, 77.1 (q, *J*=28.5 Hz), 51.8, 47.3, 38.7, 35.2, 29.6, 29.3, 28.5, 28.3, 25.9, 25.8; ^{19}F NMR (235.3 MHz, $CDCl_3$) δ: −76.3 (s, 3F); MS (DIS EI 70 eV) *m/z* (%): 653 [M+H$^+$] (5), 553 (40), 91 (100); HRMS *m/z* 652.3078 (calculated 652.3073, $C_{32}H_{43}F_3N_4O_7$).

Compound **19**: white solid; R_f 0.30 (EtOAc/*n*-Hex 1:1); $[\alpha]_D^{23}$ +11.7 (*c* 0.9, $CHCl_3$); FTIR (microscope): ν_{max}=3379, 1687, 1650, 1535 cm^{-1}; ^{1}H NMR (400 MHz, $CDCl_3$) δ: 8.10 (d, *J*=8.6 Hz, 1H), 7.43–7.05 (m, 11H), 6.07 (br s, 1H), 6.01 (d, *J*=4.1 Hz, 1H), 4.81 (d, *J*=10.6 Hz, 1H), 4.75 (d, *J*=10.6 Hz, 1H), 4.05 (d, *J*=8.9 Hz, 1H), 3.01 (dd, *J*=11.3, 3.4 Hz, 1H), 2.56 (m, 5H), 2.02–1.50 (m, 4H), 0.99 (s, 9H); ^{13}C NMR (100.6 MHz, $CDCl_3$) δ: 170.3, 169.7, 168.1, 141.4, 134.6, 129.3, 128.9, 128.6, 128.4, 128.3, 126.0, 123.1 (q, *J*=287.1 Hz), 79.2 (q, *J*=27.7 Hz), 78.5, 62.2, 44.2, 35.6, 34.6, 29.7, 28.9, 26.7, 26.1; ^{19}F NMR (235.3 MHz, $CDCl_3$) δ: −74.3 (s, 3F); MS (DIS EI 70 eV) *m/z* (%): 552 [M+H$^+$] (100).

3.10. Synthesis of hydroxamates 14a–c and 20. General procedure

To a solution of **13a** (50 mg, 0.09 mmol) in MeOH (5 mL), a catalytic amount of $Pd(OH)_2$/C was added and the reaction mixture was vigorously stirred under hydrogen atmosphere at rt for 1 h. The palladium powder was filtered over a Celite pad and the residue was washed with MeOH. The solvent was removed in vacuo and the residue was purified by FC ($CHCl_3$/MeOH 97:3), affording 36 mg of **14a** (87% yield), as a white solid: R_f 0.44 (EtOAc/*n*-Hex 1:1); $[\alpha]_D^{23}$ −29.6 (*c* 1.3, MeOH); ^{1}H NMR (400 MHz, CD_3OD) δ: 7.26–7.09 (m, 5H), 4.20 (s, 1H), 3.28 (m, 1H), 2.62 (s, 4H), 2.58–2.48 (m, 1H), 1.81–1.71 (m, 2H), 1.68–1.46 (m, 2H), 0.97 (s, 9H); ^{13}C NMR (100.6 MHz, CD_3OD) δ: 175.2, 173.6, 166.9, 144.1, 130.2, 130.1, 127.7, 125.8 (q, *J*=287.6 Hz), 80.5 (q, *J*=28.1 Hz), 64.9, 39.2, 37.5, 36.0, 30.8, 28.9, 28.0, 26.7; ^{19}F NMR (235.3 MHz, CD_3OD) δ: −73.0 (s, 3F); MS (DIS EI 70 eV) *m/z* (%): 462 [M+H$^+$] (10), 91 (30), 86 (100); HRMS *m/z* 461.2131 (calculated 461.2130, $C_{21}H_{30}F_3N_3O_5$).

Compound **14b**: white solid; R_f 0.31 (EtOAc/*n*-Hex 7:3); $[\alpha]_D^{23}$ −17.4 (*c* 0.9, MeOH); FTIR (microscope): ν_{max}=3215, 1654, 1546 cm^{-1}; ^{1}H NMR (400 MHz, $CDCl_3$) δ: 7.27–7.06 (m, 7H), 6.85 (d, *J*=8.7 Hz, 2H), 4.48 (t, *J*=7.4 Hz, 1H), 3.71 (s, 3H), 3.08 (dd, *J*=10.4, 4.1 Hz, 1H), 2.99 (dd, *J*=13.9, 7.7 Hz, 1H), 2.88 (dd, *J*=13.9, 7.4 Hz, 1H), 2.59 (s, 3H), 2.57–2.46 (m, 2H), 1.74–1.64 (m, 2H), 1.54–1.43 (m, 2H); ^{13}C NMR (100.6 MHz, $CDCl_3$) δ: 174.4, 173.9, 166.6, 160.7, 143.7, 131.8, 130.7, 129.9, 129.8, 127.4, 125.5 (q, *J*=285.9 Hz), 115.5, 80.1 (q, *J*=27.1 Hz), 57.2, 56.2, 38.6, 37.1, 30.9, 30.4, 28.3, 26.7; ^{19}F NMR (235.3 MHz, $CDCl_3$) δ: −73.4 (s, 3F); MS (DIS EI 70 eV) *m/z* (%): 526 [M+H$^+$] (5), 191 (100); HRMS *m/z* 525.2082 (calculated 525.2079, $C_{25}H_{30}F_3N_3O_6$).

Compound **14c**: white solid; R_f 0.22 (EtOAc/*n*-Hex 7:3); $[\alpha]_D^{23}$ −25.2 (*c* 1.9, MeOH); ^{1}H NMR (400 MHz, CD_3OD) δ: 7.28–7.07 (m, 5H), 4.38–4.27 (m, 1H), 3.20 (dd, *J*=10.9, 3.7 Hz, 1H), 3.11–2.96 (m, 2H), 2.66 (s, 3H), 2.64–2.51 (m, 2H), 1.85–1.55 (m, 6H), 1.47 (m, 2H), 1.42 (s, 9H); ^{13}C NMR (62.9 MHz, CD_3OD) δ: 174.7, 174.4, 166.7, 158.8, 143.5, 129.7, 129.6, 127.1, 124.4 (q, *J*=286.7 Hz), 80.1, 79.7 (q, *J*=29.6 Hz), 62.4, 54.4, 40.9, 36.8, 30.5, 30.3, 29.1, 27.7, 27.4, 26.5; ^{19}F NMR (235.3 MHz, CD_3OD) δ: −72.9 (s, 3F); MS (DIS EI 70 eV) *m/z* (%): 563 [M+H$^+$] (5), 114 (45), 91 (100); HRMS *m/z* 562.2600 (calculated 562.2605, $C_{25}H_{37}F_3N_4O_7$).

Compound **20**: white solid; R_f 0.24 (EtOAc/*n*-Hex 7:3); $[\alpha]_D^{23}$ +1.8 (*c* 0.9, MeOH); ^{1}H NMR (400 MHz, CD_3OD) δ: 7.29–7.07 (m, 5H), 4.15 (s, 1H), 2.86 (dd, *J*=11.4, 3.0 Hz, 1H), 2.70 (s, 3H), 2.69–2.62 (m, 2H), 2.61–1.51 (m, 4H), 0.97 (s, 9H); ^{13}C NMR (100.6 MHz, CD_3OD) δ: 172.4, 170.2, 168.3, 142.9, 129.4, 129.3, 126.8, 124.9 (q, *J*=286.7 Hz), 79.7 (q, *J*=26.9 Hz), 63.2, 46.7, 36.5, 35.5, 30.1, 27.4, 27.2, 26.1; ^{19}F NMR (235.3 MHz, CD_3OD) δ: −73.5 (s, 3F); MS (DIS EI 70 eV) *m/z* (%): 462 [M+H$^+$] (8), 446 (18), 99 (40), 86 (100).

3.11. X-ray structure analysis of 8x

A colorless crystal with approximate dimensions 0.25×0.3×0.4 mm was used. Hexagonal, space group $P6_5$, *a*=13.038(1), *b*=13.038(1), *c*=28.066(4) Å, *V*=4131.7(7) Å^3, *Z*=6, D_c=1.260 g cm^{-3}, μ=0.844 mm^{-1}, Bruker P4 diffractometer with graphite monochromated Cu Kα radiation (λ=1.54179 Å), $\omega/2\theta$ scan technique, room temperature, a total of reflections 6037 (2541 unique, R_{int}=0.072) collected up to 2θ=134.0°. The structure was solved by direct methods[18] and refined[19] against F^2, the amide and the hydroxyl hydrogen atoms were determined from Fourier difference maps and refined, as the other H atoms, in riding mode.

R_1=0.0414 (R_w=0.098) for 1952 observed reflections [$I \geq 2\sigma(I)$], 336 parameters refined, R_1=0.0585 (R_w=0.1074) for all data, goodness of fit=1.012, residual electron density of 0.164 and −0.118 e Å^{-3}. The value of the Flack index[20] is 0.0(3) for space group $P6_5$ and 0.2(3) for space group $P6_1$. Although hardly significant it points to the correct enantiomer that can be readily identified since L-alanine was used in the synthesis of **8x**.

3.12. Biological assays

3.12.1. Zymographic analysis. Tfm-hydroxamates **14a–c** and **20** were dissolved in EtOH to yield 10^{-1} M stock and further diluted in test solutions. Subconfluents human melanoma cells WM983A were incubated in serum free medium for 24 h. The conditioned medium containing pro-MMP-9 and pro-MMP-2 was then analyzed by zymography. Samples in 70 mM Tris–HCl pH 6.8, 10% glycerol, 2% SDS, and 0.01% bromophenol blue were applied to SDS–polyacrylamide (8%) gels co-polymerized with 1 mg/mL gelatin. After electrophoresis, gels were washed three times for 20 min with 2.5% Triton X-100 at room temperature and incubated overnight in 50 mM Tris–HCI, pH 7.5, 5 mM $CaCl_2$, 150 mM NaCl, and 0.02% Brij-35 at 37 °C in the presence or not of Tfm-hydroxamates. Gels were then stained with 0.5% Coomassie blue in 25% methanol and 10% acetic acid, and destained in the same solution without Coomassie blue. Gel images were acquired with a Duoscan T1200 scanner (AGFA), and the levels of MMPs were quantified by the Image-Pro Plus 4.1 program. The results were expressed in arbitrary units (IOD) and the IC_{50} was calculated.

3.13. Molecular modeling

Ab initio quantum chemical calculations on the active site models were performed using hybrid density functional theory (HDFT) at the B3LYP/6-31G* level,[21] using the GAMESS-USA program.[22] Geometries were fully optimized in vacuo, without any restraints.

Molecular dynamics simulations of the inhibitors were performed with the DYNAMO program[23] using a hybrid QM/MM description. Inhibitors **A** and **1** [R^1=$CH_2CH(CH_3)_2$, R^2=4-CH_3O–$C_6H_4CH_2$, R^3=CH_3] were fully solvated in a large box of water molecules and simulated in the NVT ensemble at 300 K for over 10 ns. The PM3 semiempirical method[24] was used to describe the hydroxamate and the neighboring P1 group (including –CH_3 or –CF_3) of the inhibitors. This was done in order to avoid any parametrization of these non-standard functional groups. The TIP3P water model and the OPLS-AA force field were used to describe the remaining atoms.[25] The interface between the MM and QM regions of the inhibitors was treated by the link-atom method.[23] The PM3 method including the recent re-parametrization for Zn by Merz and co-workers[24c] was used also to describe the protein active site (Zn^{2+} ion and the three hystidine rings) in our MD simulations of the protein-inhibitor complexes. The conformational free energy profiles (or potential of mean force) of the inhibitors in water were computed by umbrella sampling and subsequent WHAM analysis.[26] In particular, we applied harmonic restraints on one torsion angle, centered at values spaced by 30° [force constant 0.035 kJ/(mol deg^2), 1 ns MD simulations for each harmonic window].

Acknowledgements

We are grateful to Giorgio Colombo (CNR Milano) and Martin J. Field (IBS Grenoble) for discussions on molecular modeling. We thank the European Commission (IHP Network grant 'FLUOR MMPI' HPRN-CT-2002-00181, Integrated Projects 'STROMA' LSHC-CT-2003-503233 and 'CANCERDEGRADOME' LSHC-CT-2003-503297), MIUR (Cofin 2002, Project 'Peptidi Sintetici Bioattivi'), Politecnico di Milano, and C.N.R. for economic support. Part of the computer time for the molecular modeling studies was made available by Cilea (Milano).

Supplementary data

Supplementary data associated with this article can be found in the online version, at doi:10.1016/j.tet.2006.08.036

References and notes

1. *Biomedical Frontiers of Fluorine Chemistry*; Ojima, I., McCarthy, J. R., Welch, J. T., Eds.; ACS Books; American Chemical Society: Washington, DC, 1996.
2. Banks, R. E.; Tatlow, J. C.; Smart, B. E. *Organofluorine Chemistry: Principles and Commercial Applications*; Plenum: New York, NY, 1994.
3. (a) Coussens, L. M.; Fingleton, B.; Matrisian, L. M. *Science* **2002**, *295*, 2387–2392; (b) Whittaker, M.; Floyd, C. D.; Brown, P.; Gearing, A. J. H. *Chem. Rev.* **1999**, *99*, 2735–2776; (c) Bode, W.; Huber, R. *Biochim. Biophys. Acta* **2000**, *1477*, 241–252; (d) Giavazzi, R.; Taraboletti, G. *Crit. Rev. Oncol. Hematol.* **2001**, *37*, 53–60.
4. Becker, D. P.; DeCrescenzo, G.; Freskos, J.; Getman, D. P.; Hockerman, S. L.; Li, M.; Mehta, P.; Munie, G. E.; Swearingen, C. *Bioorg. Med. Chem. Lett.* **2001**, *11*, 2723–2725.
5. (a) Jacobson, I. C.; Reddy, P. G.; Wasserman, Z. R.; Hardman, K. D.; Covington, M. B.; Arner, E. C.; Copeland, R. A.; Decicco, C. P.; Magolda, R. L. *Bioorg. Med. Chem. Lett.* **1998**, *8*, 837–842; (b) Jacobson, I. C.; Reddy, G. P. *Tetrahedron Lett.* **1996**, *37*, 8263–8266.
6. However, it should be noted that the hydrogen bond involving the quaternary OH and the Glu-202 of MMP-3 is not present in the X-ray structure of the complex with the **A** analog having R^1=$CH_2CH(CH_3)_2$.
7. Humphrey, W.; Dalke, A.; Schulten, K. *J. Mol. Graphics* **1996**, *14*, 33–38.
8. Zanda, M. *New J. Chem.* **2004**, *28*, 1401–1411.
9. For a communication on this work see: Sani, M.; Belotti, D.; Giavazzi, R.; Panzeri, W.; Volonterio, A.; Zanda, M. *Tetrahedron Lett.* **2004**, *45*, 1611–1615.
10. Zucca, C.; Bravo, P.; Malpezzi, L.; Volonterio, A.; Zanda, M. *J. Fluorine Chem.* **2002**, *114*, 215–223.
11. (a) Crimmins, M. T.; King, B. W.; Tabet, E. A.; Chaudhary, K. *J. Org. Chem.* **2001**, *66*, 894–902; (b) Crimmins, M. T.; McDougall, P. J. *Org. Lett.* **2003**, *5*, 591–594 and references therein; (c) Palomo, C.; Oiarbide, M.; García, J. M. *Chem.—Eur. J.* **2002**, *8*, 37–44.

12. Su, D.-W.; Wang, Y.-C.; Yan, T.-H. *Tetrahedron Lett.* **1999**, *40*, 4197–4198.
13. CCDC 601635 contains the supplementary crystallographic data for this paper. These data can be obtained free of charge via www.ccdc.cam.ac.uk/conts/retrieving.html (or from the CCDC, 12 Union Road, Cambridge CB2 1EZ, UK; fax: +44 1223 336033; e-mail: deposi@ccdc.cam.ac.uk).
14. Carpino, L. A.; El Faham, A. *J. Org. Chem.* **1995**, *60*, 3561–3564 and references therein.
15. Humphrey, J. M.; Chamberlin, A. R. *Chem. Rev.* **1997**, *97*, 2243–2266.
16. (a) Gorecka, A.; Leplawy, M.; Zabrocki, J.; Zwierzak, A. *Synthesis* **1978**, 474–476. Contrary to the statement of these authors, $BrPO(OEt)_2$ undergoes rapid decomposition even at 4 °C, therefore it must be used within 1–2 h from its preparation. Our results are in agreement with an earlier report: (b) Goldwhite, H.; Saunders, B. C. *J. Chem. Soc.* **1955**, 3564.
17. For the addition of amine nucleophiles to β-lactones see: Nelson, S. G.; Spencer, K. L.; Cheung, W. S.; Mamie, S. J. *Tetrahedron* **2002**, *58*, 7081–7091.
18. Altomare, A.; Burla, M. C.; Camalli, M.; Cascarano, G. L.; Giacovazzo, C.; Guagliardi, A.; Moliterni, A. G. G.; Polidori, G. P.; Spagna, R. *J. Appl. Crystallogr.* **1999**, *32*, 115–119.
19. Sheldrick, G. M. *SHELXL-97. Program for the Refinement of Crystal Structures*; University of Göttingen: Göttingen, Germany, 1997.
20. Flack, H. D. *Acta Crystallogr., Sect. A* **1983**, *39*, 876–881.
21. (a) Hehre, W. J.; Radom, L.; Schleyer, P. v. R.; Pople, J. A. *Ab Initio Molecular Orbital Theory*; Wiley: New York, NY, 1986; (b) Koch, W.; Holthausen, M. C. *A Chemist's Guide to Density Functional Theory*; Wiley-VCH: Weinheim, 2000.
22. Schmidt, M. W.; Baldridge, K. K.; Boatz, J. A.; Elbert, S. T.; Gordon, M. S.; Jensen, J. H.; Koseki, S.; Matsunaga, N.; Nguyen, K. A.; Su, S. J.; Windus, T. L.; Dupuis, M.; Montgomery, J. A. *J. Comput. Chem.* **1993**, *14*, 1347–1363.
23. (a) Field, M. J. *A Practical Introduction to the Simulation of Molecular Systems*; Cambridge University Press: Cambridge, 1999; (b) Field, M. J.; Albe, M.; Bret, C.; Proust-De Martin, F.; Thomas, A. *J. Comput. Chem.* **2000**, *21*, 1088–1100.
24. (a) Stewart, J. J. P. *J. Comput. Chem.* **1989**, *10*, 209–220; (b) Stewart, J. J. P. *J. Comput. Chem.* **1989**, *10*, 221–264; (c) Brothers, E. N.; Suarez, D.; Deerfield, D. W., II; Merz, K. M., Jr. *J. Comput. Chem.* **2004**, *25*, 1677–1692.
25. Jorgensen, W. L.; Maxwell, D. S.; Tirado-Rives, J. *J. Am. Chem. Soc.* **1996**, *115*, 11225–11235.
26. Roux, B. *Comput. Phys. Commun.* **1995**, *91*, 275–282.